Available online at www.sciencedirect.com
SCIENCE DIRECT
Biochemical Pharmacology 70 (2005) 1642–1652
Biochemical Pharmacology
www.elsevier.com/locate/biochempharm

Novel potential neuroprotective agents with both iron chelating and amino acid-based derivatives targeting central nervous system neurons

Hailin Zheng [a], Moussa B.H. Youdim [b], Lev M. Weiner [c], Mati Fridkin [a,*]

[a] *Department of Organic Chemistry, The Weizmann Institute of Science, Herzl St., Rehovot 76100, Israel*
[b] *Eve Topf and USA National Parkinson Foundation Centers of Excellence for Neurodegenerative Diseases and Department of Pharmacology, Technion-Appaport Family Faculty of Medicine, Haifa 31096, Israel*
[c] *Chemical Research Support, The Weizmann Institute of Science, Rehovot 76100, Israel*

Received 19 July 2005; accepted 12 September 2005

Abstract

Antioxidants and iron chelating molecules are known as neuroprotective agents in animal models of neurodegenerative disorders such as Alzheimer's disease (AD) and Parkinson's disease (PD). In this study, we designed and synthesized a novel bifunctional molecule (M10) with radical scavenging and iron chelating ability on an amino acid carrier likely to be a substrate for system L, thus targeting the compound to the central nervous system (CNS). M10 had a moderate iron affinity in HEPES buffer (pH 7.4) with log $K_3 = 12.25 \pm 0.55$ but exhibited highly inhibitory action against iron-induced lipid peroxidation, with an IC_{50} value (12 μM) comparable to that of desferal (DFO). EPR studies indicated that M10 was a highly potent $^{\bullet}OH$ scavenger with an IC_{50} of about 0.3 molar ratio of M10 to H_2O_2. In PC12 cell culture, M10 was at least as potent as the anti-Parkinson drug rasagiline in protecting against cell death induced by serum-deprivation and by 6-hydroxydopamine (6-OHDA). These results suggest that M10 deserves further investigation as a potential agent for the treatment of neurodegenerative disorders such as AD and PD.

Keywords: Antioxidant; Iron chelator; Lipid peroxidation; Neurodegenerative diseases; Neuroprotection; Oxidative stress

1. Introduction

Neurodegeneration in Alzheimer's disease (AD), Parkinson's disease (PD), amyotrophic lateral sclerosis (ALS) and Huntington disease (HD) is associated with a cascade of events. The major pathogenic events include iron-induced oxidative stress, increased levels of iron, inflammatory processes and depletion of antioxidants in the brain [1–4]. In the past decade, a large number of antioxidants such as Vitamin E, ebselen, carotenoids, favonoids, lipoic acid and lazaroid have been investigated as potential therapeutic agents to control oxidative stress in neurodegenerative disorders [5–7]. Although such compounds have shown neuroprotection when used in animal models or in small clinical studies, their use is still relatively limited mainly because of poor bioavailability and/or inadequate antioxidant property under physiological conditions [7]. Because of toxicity concerns, less effort has been devoted to decreasing oxidative stress by using metal chelators to control the levels of iron, which at high levels, has been implicated in converting the less reactive hydrogen peroxide into the highly toxic hydroxyl radical.

Iron levels are clearly elevated at the site where neurons degenerate in neurodegenerative diseases such as PD, AD and HD [8]. For example, in PD there is selective increase of iron in substantia nigra pars compacta (SNPC) [9] and within the melanized dopamine neurons [4,10]. Iron in SNPC also accumulates in the proliferated reactive microglia, astrocytes and oligodendrocytes [13]. In AD, iron accumulation occurs in microglia and oligodendrocytes within plaques and tangle-bearing neurons [14]. In other neurodegenerative diseases, such as HD, ALS and multiple sclerosis, iron also accumulates at the site of the lesion and is thought to participate in the neurodegenerative process [14]. The increased level of iron in the brain could induce

* Corresponding author. Tel.: +972 8 934 2505; fax: +972 8 934 4142.
E-mail address: mati.fridkin@weizmann.ac.il (M. Fridkin).

0006-2952/$ – see front matter © 2005 Elsevier Inc. All rights reserved.
doi:10.1016/j.bcp.2005.09.003

and exacerbate oxidative stress [15,16], promote deposition of amyloid-β (Aβ) [17] and also be closely linked to the proliferation of the reactive microglia and the inflammatory responses, as observed in neurotoxin-induced neurodegeneration and neurodegenerative diseases [18]. In view of these, iron is thought to play a pivotal role in the pathogenesis of PD and other neurodegenerative diseases. Because of the iron-mediated toxicity and its participation in the Fenton reaction to continually produce free radicals, the efficacy of an antioxidant in reducing oxidative stress could be undermined. This may explain, at least in part, why many antioxidants fail to provide neuroprotection in the clinic although they all show neuroprotective activity in animal models.

Recent studies have shown that iron chelators can offer neuroprotection both in vitro and in vivo. For example, intracereventricularly (ICV) injected desferal (DFO), an iron chelator drug used for treating iron overload, protects against the dopaminergic neurodegeneration induced by 6-hydroxydopamine (6-OHDA) [19], and prevents iron and 1-methyl-4-phenyl-1,2,5,6-tetrahydropyridinium (MPTP)-induced neurotoxicity in mice [20]. An antibiotic iron chelator, 5-chloro-7-iodo-8-hydroxyquinoline (clioquinol), provides neuroprotection against MPTP-induced neurotoxicity in vivo [21]. Oral administration of clioquinol inhibits β-amyloid accumulation in an AD transgenic mouse model via its metal chelating property [22]. Unfortunately, clioquinol was withdrawn from the market because of its high toxicity [23], and desferal has no oral activity coupled with cytotoxicity [24].

Iron chelators for clinical use in neurological disorders should cross the blood–brain barrier (BBB) and possess strong iron chelating ability for removal of excess iron in the brain. Increasing the lipophilicity of a chelator may improve its penetration through the BBB, but its uptake into other non-related tissues (cells) may likewise increase. Entrance of strong lipophilic iron chelators into cells is expected to interact with essential iron containing enzymes such as ribonucleotide reductase and tyrosine hydroxylase and thus promote undesirable side effects, especially when administered for prolonged periods of time [25,26]. Therefore, it is of interest to develop new chelators that selectively target the brain to help circumvent some limitations of currently available iron chelators.

We have recently developed a number of novel iron chelators [27,28]. VK28 and M30 (Fig. 1), two representatives of this novel class of iron chelators, have been shown to have neuroprotective activity in vivo against 6-OHDA and in vivo against MPTP neurotoxicity [29,30,39,40]. VK28 and M30, like clioquinol, are non-selective iron chelators with good permeability into both the brain and normal cells [29,30]. We therefore designed and synthesized a novel antioxidant-iron chelator, designated M10 (Fig. 1), derived from VK28, M30 and clioquinol but with potential selective targeting to the brain. M10 has two important attributes: first, it is a water-soluble molecule with high hydrophilicity that would help prevent it from penetrating into cells to interfere with the normal iron metabolism and thus possibly reduce the drug toxicity; second, M10 possesses a neutral amino acid carrier group that is a substrate for the uptake system L thus targeting it to the brain. A number of hydrophilic drugs are known to be transported into the brain via system L, including L-DOPA, α-methyl-DOPA, melphalan, 6-diazo-5-oxo-L-norleucine, acivicin and SDZ EAB 515 (Fig. 1) [31–34].

M10 or L-3-(8-hydroxyquinolin-5-yl)alanine is an oxine-derived amino acid. Some oxine-derived amino acid analogs have been developed for use as potential fluorescent chemosensors of divalent zinc [11,12]. In this paper, we report for the first time the synthesis and preliminary characterization of the novel antioxidant chelator L-3-(8-hydroxyquinolin-5-yl)alanine (M10).

2. Materials and methods

2.1. Chemicals and routine equipment

Unless otherwise stated, all chemicals were obtained from commercial suppliers (Sigma–Aldrich, Merck, or

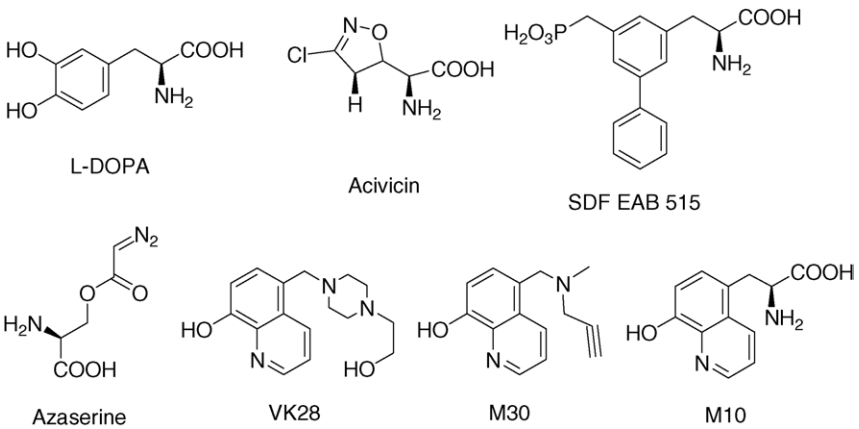

Fig. 1. Structures of VK28, M30, M10 and some known drugs with a neutral amino acid carrier.

Fluka). Proton NMR spectra were measured on a Bruker DPX-250 spectrometer (Bruker, Karlsruhe, Germany). Rasagiline was kindly donated by Teva Pharmaceuticals Ltd. (Petach-Tikva, Israel). Flash column chromatography separations were performed on silica gel Merck 60 (230–400 mesh ASTM, Merck KGaA, Darmstadt, Germany). UV–vis spectra were measured on a Beckman DU 7500 spectrophotometer (Beckman Coulter, Inc., Fullerton, CA, USA). TLC was performed on Merck Kieselgel 60 F_{254} plates (Merck KGaA). Mass spectra (DI, EI-MS) were measured on a VG-platform-II electrospray single quadropole mass spectrometry (Micro Mass, UK). D- and L-isomers were separated by preparative HPLC, performed on a Waters system composed of two model 510 pumps, model 680 automated gradient controller and model 441 absorbance detector (Waters, Milford, MA). The column effluents were monitored by UV absorbance at 254 nm. HPLC pre-packed columns were Vydac RP-18 columns (250 mm × 22 mm; 10 μm bead size, Merck, Darmstadt, Germany) for preparative purifications and Lichrospher100 RP-18 (250 mm × 4 mm; 5 μm bead size, Merck) for analytical purposes. HPLC purification was achieved by using 0.1% TFA in water as A and 0.1% TFA in 75% acetonitrile in water (v/v) as B.

2.2. Synthesis of L-3-(8-hydroxyquinolin-5-yl)alanine L- (M10) and D (M9)-isomers

The novel antioxidant chelators L-3-(8-hydroxyquinolin-5-yl)alanine (M10) and its D-isomer (M9) were prepared as detailed below and as summarized in Scheme 1.

2.2.1. 5-Chloromethyl-8-quinolinol hydrochloride (2)

A mixture of 14.6 g (0.1 mole) of 8-quinolinol, 16 ml of 32% hydrochloric acid and 16 ml (0.1 ml) of 37% formaldehyde at 0 °C was treated with hydrogen chloride gas (100% HCl) for 6 h. The solution was allowed to stand at room temperature (RT) for 2 h without stirring. The yellow solid was collected on a filter and dried to give 16 g crude 5-chloro-methyl-8-quinolinol hydrochloride **2**. H^1 NMR (250 MHz, $CDCl_3$): 5.32 (s, 2H), 7.53 (m, 1H), 7.85 (m, H), 8.12 (m, 1H), 9.12 (m, 1H), 9.28 (m, 1H).

2.2.2. 8-(5-Chloromethyl)quinolyl acetate (3)

To a stirred solution of crude 5-chloromethyl-8-quinolinol hydrochloride **2** (230 mg, 1 mmole) in dry DMF (5 ml) at 0 °C were added slowly and simultaneously pyridine (0.3 ml, 2.5 mmole) and acetyl chloride (0.6 ml, 8 mmole) under N_2 protection. The reaction mixture was stirred at 0 °C for 1 h at RT for 1 h. After cooling to 0 °C, 10 ml of water was added, and the resulting mixture was stirred at 0 °C for 20 min. The mixture was extracted with chloroform (3× 20 ml). The combined organic layer was washed with saturated $NaHCO_3$ (2× 20 ml) and brine solution (2× 20 ml) and dried over Na_2SO_4. Evaporation afforded the title compound **3** (crude) (180 mg, 75%) as a light brown solid. mp = 119–120 °C, ^{1}H NMR (250 MHz, $CDCl_3$): 2.25 (s, 3H), 4.98 (s, 2H), 7.40 (d, J = 7.7 Hz, 1H), 7.55 (m, 2H), 8.47 (dd, J = 8.6, 1.6 Hz, 1H), 8.96 (dd, J = 4.2, 1.5 Hz, 1H).

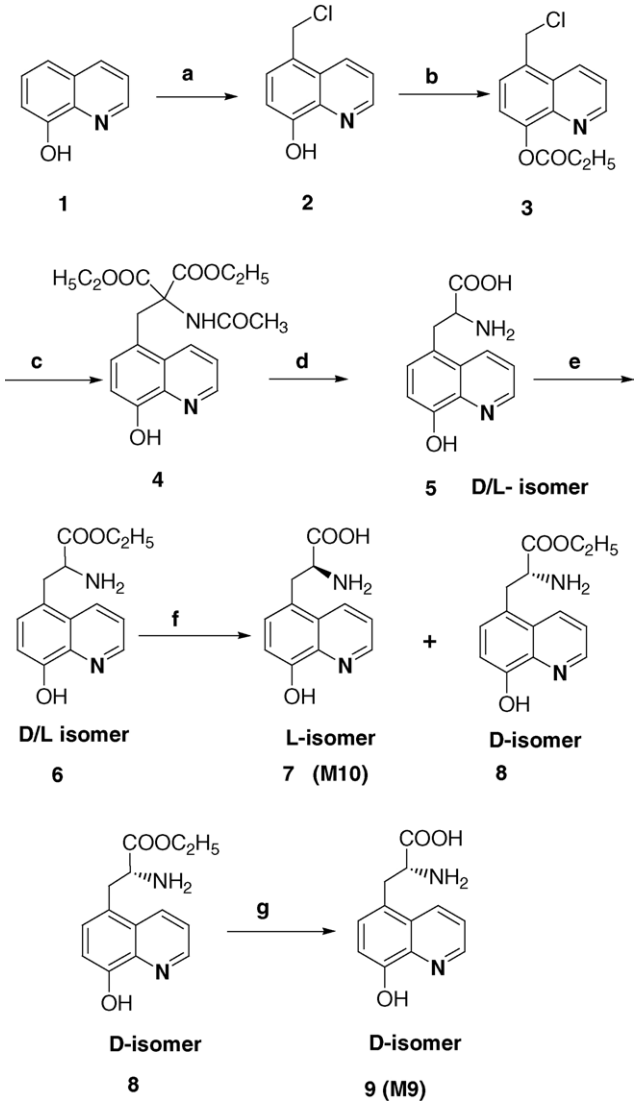

Scheme 1. Reagents and conditions: (a) HCl (32%), HCHO (37%), 0 → RT, 8 h, 70%. (b) CH_3COCl, pyridine, DMF, 0 °C → RT, 2 h, 75%. (c) Na, ethanol, acetamidomalonate, reflux 5 h, 59%. (d) 6N HCl reflux 8 h. (e) EtOH, $SOCl_2$ reflux 6 h. (f) α-Chymotrypsin pH 6.0–6.5, 2 h RT; 35% L-acid and 88% (recovery) D-ester. (g) 0.2 M NaOH RT, 6 h.

2.2.3. Diethyl (8-hydroxyquinolin-5-yl-methyl)-acetamidomalonate (4)

A solution of acetamidomalonate (183 mg, 0.842 mmole) and metallic sodium (34 mg, 0.842 mmole) in ethanol was added to a solution of 8-(5-chloromethyl)-quinolyl acetate **3** (180 mg, 0.765 mmole). The resultant mixture was stirred for 5 h under reflux, cooled and evaporated in vacuum. To the residue was added water

(20 ml) and the mixture was extracted with $CHCl_3$/EtOAc (3× 20 ml, 1:1). The organic layer was washed with brine (2× 20) and dried over Na_2SO_4. Evaporation afforded the title compound **4** (170 mg, 59%) as a light brown solid (crude) mp = 153–154 °C, R_f: 0.25 ($CHCl_3$:MeOH:NH_3, 9:1:0.25), ^{1}H NMR (250 MHz, $CDCl_3$): 1.30 (dd, J = 7.1, 7.1 Hz, 6H), 1.86 (s, 3H), 4.03 (s, 2H), 4.27 (m, 4H), 6.46 (s, 1NH), 7.10 (dd, J = 16.6, 7.9 Hz, 2H), 7.42 (dd, J = 8.7, 4.2 Hz, 1H), 8.76 (dd, J = 4.2, 1.1 Hz, 1H).

2.2.4. DL-3-(8-Hydroxyquinolin-5-yl)alanine (5)

Diethyl (8-hydroxyquinolin-5-yl-methyl)-acetamidomalonate **4** (8.9 g, 21.9 mmole) was dissolved in 6N HCl (150 ml) and the resultant mixture was refluxed for 10 h. The reaction mixture was evaporated to dryness by removing the solvent in vacuum. The residue was redissolved in H_2O and filtered. The pH of the solution was adjusted to 5–5.5 with 10% NaOH. A yellow precipitate was collected by filtration, washed thoroughly with water, re-crystallized from water (pH 5.5) and washed with acetone to give DL-3-(8-hydroxy quinolin-5-yl)alanine **5** (3.8 g, yield 65%) of 100% purity, checked by HPLC [C_{18}; solvent A = water, 0.1%, v/v, TFA; solvent B = MeCN:water = 3:1, 0.1%, v/v, TFA; t_R = 18.2 min (linear gradient 0–80% B over 55 min)]. mp = 194 °C (decompose). ^{1}H NMR (250 MHz, D_2O) 3.42 (m, 1H), 3.58 (m, 1H), 3.93 (dd, J = 7.2, 7.2 Hz, 1H), 7.22 (d, J = 8.0 Hz, 1H), 7.50 (d, J = 8.1 Hz, 1H), 7.94 (dd, J = 8.7, 5.4 Hz, 1H), 8.84 (d, J = 5.1 Hz, 1H)., 9.06 (d, J = 8.7 Hz, 1H); ^{13}C NMR (100 MHz, DMSO) 32.14, 53.11, 111.03, 121.27, 127.46., 129.76, 133.35, 138.13, 147.46, 152.55, 170.30. Mass spectrometry: calculated for $C_{12}H_{12}N_2O_3$ m/z $[M + H]^+$ = 233.24, found $[M + H]^+$ = 233.25.

2.2.5. DL-3-(8-Hydroxyquinolin-5-yl)alanine ethyl ester (6)

To a stirred slurry of DL-3-(8-hydroxyquinolin-5-yl)alanine **5** (2.19 g, 7.04 mmole) in absolute ethanol (26 ml) at 0 °C, protected from atmospheric moisture by $CaCl_2$ tube in N_2, was added dropwise thionyl chloride (1.1 ml, 4.1 mmole). The reaction mixture was stirred at 0 °C for 30 min, and at RT for 30 min, and then refluxed overnight. The solution was evaporated to dryness in vacuum. The residue was dissolved in absolute ethanol and evaporated to dryness. To ensure completeness of the esterification, the whole procedure was repeated. The ester **6** (yellow solid, 1.67 g, 92% yield), shown by HPLC to contain about 1% free amino acids, was further purified by Flash column chromatography (CH_2Cl_2:MeOH:AcOH, 9:1.5:1.5). ^{1}H NMR (250 MHz, D_2O) 0.94 (dd, J = 7.2, 7.2 Hz, 3H), 3.63 (m, 2H), 4.01 (m, 2H), 4.34 (dd, J = 7.7, 7.5 Hz, 1H), 7.31 (d, J = 8.0 Hz, 1H), 7.56 (d, J = 8.2 Hz 1H), 8.01 (dd, J = 8.7, 5.4 Hz, 1H), 8.93 (d, J = 5.4 Hz, 1H), 9.08 (d, J = 8.7 Hz, 1H).

2.2.6. L-3-(8-Hydroxyquinolin-5-yl)alanine (7 or M10) and D-3-(8-hydroxyquinolin-5-yl)alanine ethyl ester (8)

Ester **6** (89.2 mg) was dissolved in 5 ml water and the pH of the solution was adjusted to about 6.4 with 0.2 M Na OH. α-Chymotrypsin (0.9 mg) was added, and the mixture was incubated at RT for 6 h with the pH being kept constant by addition of 0.2 M NaOH. After digestion, the mixture was lyophilized to dryness and separated by preparative HPLC [C_{18}; solvent A = water, 0.1%, v/v, TFA; solvent B = MeCN:water = 3:1, 0.1%, v/v, TFA; t_R = 18.0 min (linear gradient 0–80% B over 55 min)]. L-3-(8-Hydroxyquinolin-5-yl)alanine **7** (M10) was obtained: 27.6 mg, 35%, 100% purity, $[\alpha]_D^{20}$ = +13.5 (D-ethyl ester was recovered 39.2 mg, 88% recovery). ^{1}H NMR (250 MHz, D_2O) 3.49 (m, 1H), 3.65 (m, 1H), 3.95 (m, 1H), 7.34 (m, 1H), 7.57 (m, 1H), 8.0 (m, 1H), 8.91 (m, 1H), 9.14 (m, 1H); calcd for $C_{12}H_{12}N_2O_3$ m/z $[M + H]^+$ = 233.24, found $[M + H]^+$ = 233.26.

2.2.7. D-3-(8-hydroxyquinolin-5-yl)alanine (9 or M9)

D-3-(8-Hydroxyquinolin-5-yl)alanine ethyl ester **8** (33.4 mg) was dissolved in 11 ml of 0.2 M NaOH and the solution was stirred at RT for 6 h. Water was removed by lyophilization, and the product was purified by preparative HPLC [C_{18}; solvent A = water, 0.1%, v/v, TFA; solvent B = MeCN:water = 3:1, 0.1%, v/v, TFA; t_R = 18.4 min (linear gradient 0–80% B over 55 min)] to give D-amino acid **9** or M9 26.8 mg, 89%, 99.1% purity. $[\alpha]_D^{20}$ = −10.3. ^{1}H NMR (250 MHz, D_2O) 3.40 (s, 1H), 3.55 (s, 1H), 3.91 (s, 1H), 7.15 (s, 1H), 7.45 (s, 1H), 7.91 (s, 1H), 8.80 (s, 1H), 9.02 (s, 1H), calcd for $C_{12}H_{12}N_2O_3$ m/z $[M + H]^+$ = 233.24, found $[M + H]^+$ = 233.26.

2.3. Detection of free radical intermediates

Hydroxyl radical ($^\bullet$OH) was produced by the photolysis of H_2O_2 as previously described [35]. Formation of the hydroxyl radical ($^\bullet$OH) was followed by electron spin resonance (ESR) of the spin adduct (DMPO–$^\bullet$OH). A typical 60 μl incubation mixture for trapping $^\bullet$OH radicals contained 50 mM DMPO. For H_2O_2 photolysis, the irradiation source was a KL1500 electronic projector lamp (Schott, Germany). Samples were irradiated directly inside the ESR cavity by white light with an optical fiber. The ESR spectra of DMPO–$^\bullet$OH were recorded in a Bruker electron spin resonance ER200D-SRC spectrometer (Bruker, Karlsruhe, Germany) in a quartz flat cell of 60 μl. The standard instrumental parameters were as follows: microwave frequency, 9.7 GHz; incident microwave power, 10 MW; center of the field, 3480; scan range, 100 G; field modulation, 1 G; receiver gain, 6.3×10^{-5}; and time constant, 1.3 s. The ESR spectrum of DMPO–$^\bullet$OH consisted of a quartet (1:2:2:1) with hyperfine splitting constants of $a_N = a_H$ = 14.9 G. The amplitude of the third peak in the quartet of the ESR spectrum of DMPO–$^\bullet$OH was used for further calculations.

2.4. Lipid peroxidation assay

Lipid peroxidation (LPO) was measured in rat brain mitochondrial membrane homogenates as previously described [36]. This method is based on the oxidation of polyunsaturated fatty acids in biologic membranes, giving rise to a variety of lipid breakdown products such as malondialdehyde (MDA). By reacting MDA with thiobarbituric acid (TBA) a pink pigment is formed, which can be detected by UV–vis spectroscopy. LPO was induced by 50 μM ascorbic acid and 1.5 μM $FeSO_4$. The absorption of thiobarbituric acid derivatives was measured photometrically at 532 nm.

2.5. Determination of neuroprotective effects on PC12 cells

2.5.1. PC12 cell culture

Rat PC12 cells, originating from rat pheochromocytoma, were grown at 37 °C in a humid 5% CO_2, 95% air environment in a growth medium containing Dulbecco's modified Eagle's medium (DMEM, Invitrogen, Groningen, the Netherlands) supplemented with glucose (1 mg/1 ml), 5% fetal calf serum (Bet Haemek, Israel), 10% horse serum and a 1% mixture of penicillin/streptomycin. On confluence, the culture medium was removed and the cells were detached by vigorous washing followed by centrifugation at 200 × *g* for 5 min. For experiments with serum-deprivation, cells were resuspended in DMEM with full serum content, 0.5×10^4 cells/well, and then placed in microtiter plates (96 wells) precoated with collagen (10 μg/cm^2) and allowed to attach for 24 h. Next, the medium was replaced with DMEM containing 0.1% bovine serum albumin (BSA). Drugs were added to the cells after 1 h incubation. Cells were incubated for 24 h before being subjected to the 3-(4.5-dimethylthiazol-2-yl)-2.5-diphenyltetrazolium (MTT) assays (see below). For experiments with the neurotoxin 6-hydroxydopamine, PC 12 cells (1×10^4 cells/well) in DMEM with one-third full serum content were placed in microtiter plates (96 wells) precoated with collagen (10 μg/cm^2) and allowed to attach for 24 h before treatment. Drugs were added to cells 30 min before insults with 6-hydroxy-dopamine (150 μM). Cells were incubated at 37 C for 24 h before being assayed with MTT.

2.5.2. MTT test for cell viability

The MTT test is based on the conversion of MTT to blue formasan crystals by viable cells. Briefly, 24 h after treatment, the medium was removed and replaced with a medium (100 μl/well) lacking serum. To each well, 10 μl of a 5 mg/ml MTT solution in PBS was added. After incubation at 37 °C for 2 h, 100 μl of 10% SDS in 0.01N HCl was added and the solution was mixed thoroughly and incubated for additional 24 h. Absorption was determined in a Perkin-Elmer Dual Wave-length Eliza-Reader at λ = 570 nm/650 nm after automatic subtraction of background readings. Cell viability was expressed as a percentage of cells untreated with 6-hydroxydopamine, which served as the control group and was designated as 100%. The results are expressed as percentage of the control.

2.5.3. ELISA programmed cell death detection

Cells were analyzed for apoptosis by cell death detection ELISA (Roche Applied Science, Mannheim, Germany). The assay is based on the use of mouse monoclonal antibodies to detect free histones and fragmented DNA. Briefly, after 24 h incubation with the test compounds, cells were centrifuged at 200 × *g* for 10 min, the supernatant was removed and 300 μl of lysis buffer was added to each of the cell pellets. Cells were incubated for 30 min at RT and then centrifuged again at 200 × *g* for 10 min. A supernatant aliquot (10 μl) was added along with 90 μl of the antibody mixture (containing anti-histone and anti-DNA antibodies) to each well of the streptavidin-coated 96-well plate. After 2 h incubation at RT, the reaction mixture was removed and the plate was washed with incubation buffer. The bound peroxidase was then determined photometrically at 405 nm/492 nm using 2,2′-azino-di(3-ethylbenz-thiazolinsulfonate) [ABTS] as a substrate. Cell death was expressed as a percentage of the apoptosis in the cells untreated with drugs, which served as the control group and was designated as 100%. The results are expressed as percentage of the control.

3. Statistical analysis

All assays were performed at least in triplicate and the data were expressed as mean ± S.E.M. Data were analyzed by Student's *t*-test. Variations were considered significant at $p \leq 0.05$.

4. Results

4.1. Metal chelating studies

4.1.1. Formation of metal complexes with Fe(II), Fe(III), Cu(II) and Zn(II)

UV–vis spectroscopy suggested that M10 formed complexes with Fe(III)/(II), Cu(II) and Zn(II) in HEPES buffer (pH 7.4) at 37 °C. Fig. 2 shows the absorption spectra of M10 in the absence and presence of metal ions in HEPES buffer (pH 7.4). There was a pronounced absorbance by M10 around 325 nm but no apparent absorption in the range of 370–800 nm (Fig. 2a). On addition of $FeCl_3$ to the solution of M10, three new bands around 372, 475 and 610 nm appeared along with the decrease in the 325 nm band (Fig. 2c), suggesting complex formation between M10 and Fe(III). Furthermore, there were no significant changes in absorbance of the above

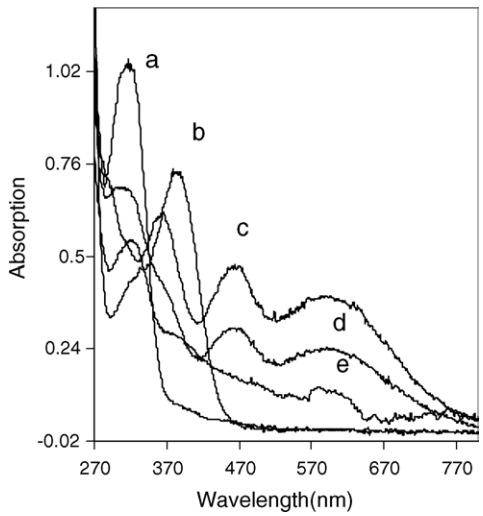

Fig. 2. Absorption spectra of M10 in the absence and presence of metal salts. Concentration of M10 = 0.2 mM. Solvent: HEPES buffer pH 7.4. Concentrations of metal salts: (a) 0.0; (b) 0.2 mM $CuSO_4$; (c) $FeCl_3$; (d) $FeSO_4$; (e) $ZnCl_2$.

metal complex solutions after incubation for 24 h at 37 °C, indicating the stability of these metal complexes in HEPES buffer (pH 7.4). Similar results were observed with M10 in the presence of Cu(II), Fe(II) and Zn(II) ions in HEPES buffer (pH 7.4) (Fig. 2b, d and e, respectively).

4.1.2. Composition of M10–metal complexes and stability constants

The composition of M10–metal complexes was determined by Job's method of continuous variations [37,38]. The experimental data suggest that in HEPES buffer (pH 7.4) at RT M10 formed metal complexes with Fe(II), Fe(III), Cu(II) and Zn(II) at a ratio (ligand-to-metal) of 1:1, 3:1, 2:1 and 2:1, respectively. The composition of M10–Fe(III) was further confirmed by mass spectrometry. As shown in Fig. 3A, M10–Fe (III) complex gave ion of *m/z* 772.67, corresponding to the ion $[Fe(M10)_3 + Na]^+$ with stoichiometry of 3:1. The negative electrospray ionization spectrum of M10–Fe(III) complex (Fig. 3B) contained two peaks of low intensity at *m/z* 748.61 and 770.42, which can be explained by the complexes of 3:1 stoichiometry $[Fe(M10)_3–H]^-$ and $[Fe(M10)_3 + Na–2H]^-$.

In solution, complex formation between a ligand L and a cation M takes place as follows:

$$nL + M \rightleftharpoons ML_n \quad (1)$$

The stability constant K is given by the equation: $K_n = [ML_n]/[M][L]^n$. K_1 ($n = 1$) for Fe(II)–M10 complex, K_2 ($n = 2$) for Cu(II)–M10 and Zn(II)–M10 complexes and K_3 ($n = 3$) for Fe(III)–M10 complex. K_n was determined by the method of Foley and Anderson [38]. In this method, pairs of solutions with the same optical densities (containing equal concentrations of the complex but different total concentrations) were prepared. The concentration of the

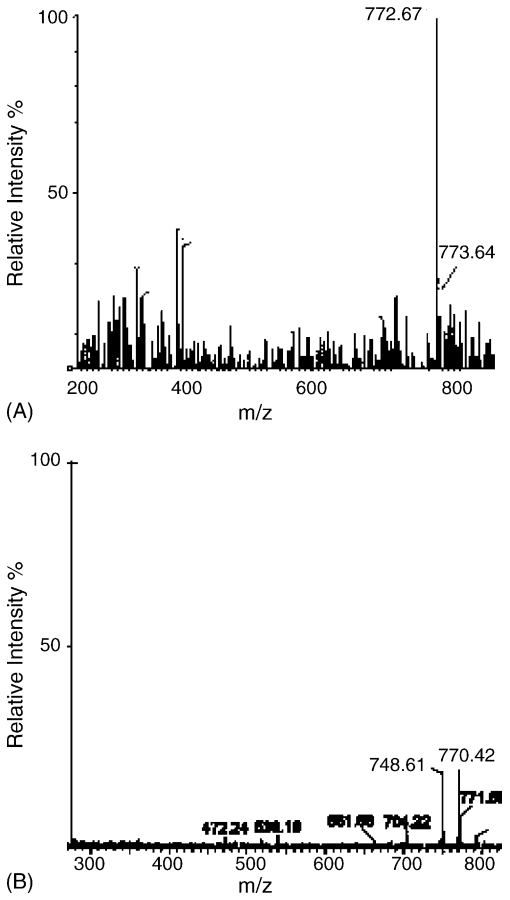

Fig. 3. (A) Positive ion electrospray ionization mass spectrum of a solution of iron(III) chloride and M10. (B) Negative ion electrospray ionization mass spectrum of a solution of iron(III) chloride and M10.

complexes, and thus the values of K_n, may be calculated from the relation:

$$K_n = \frac{x}{(a_1 - nx)^n(b_1 - x)} = \frac{x}{(a_2 - nx)^n(b_2 - x)}$$

where *a*'s and *b*'s denote initial concentration of M10 and metal–salt, respectively, and x denotes the concentration of M10–metal complex. The log K values calculated for M10 in HEPES buffer (pH 7.4) at 25 °C are 5.07 ± 0.31 [log K_1 for Fe(II)], 12.25 ± 0.55 [log K_3 for Fe(III)], 8.39 ± 0.74 [log K_2 for Cu(II)] and 7.58 ± 0.37 [log K_2 for Zn(II)].

4.2. Antioxidant property of M10 in rat brain homogenates

Imbalanced oxidative homeostasis and lipid peroxidation were implicated in neurodegenerative diseases such as AD and PD [6,15,16]. Thus, we next determined the antioxidant property of M10 in rat brain mitochondrial fraction. The oxidative process was initiated by Fe^{2+}/ascorbate. As shown in Fig. 4, M10 exhibited high potency in inhibiting lipid peroxidation as measured by the formation of malondialdehyde (MDA), with an IC_{50} of about

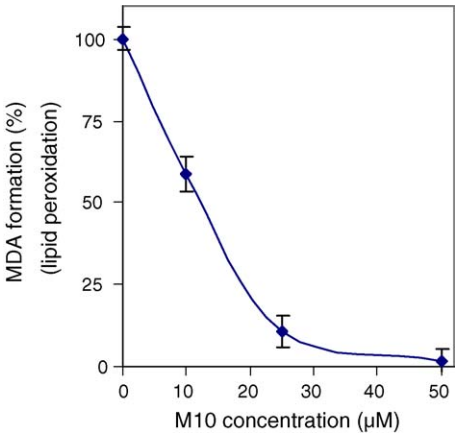

Fig. 4. Inhibition of iron-induced lipid peroxidation in rat brain homogenates by M10. TBARS formation was induced by 1.5 μM $FeSO_4$/50 μM ascorbic acid. The results are the mean ± S.E.M., $n = 3$, $p < 0.05$.

12 μM. This inhibition was comparable to that of DFO, a highly potent inhibitor of lipid peroxidation and a strong iron chelator with an IC_{50} of about 8 μM in the same experiments.

4.3. Hydroxyl radical scavenging property

The radical scavenging property of M10 was studied by electron paramagnetic resonance (EPR) spectroscopy with spin trapping technique [35,41]. Hydroxyl radical ($^{\bullet}OH$) was produced by the photolysis of H_2O_2 (reaction (2)). The resulting radicals were trapped with 5,5-dimethyl-pyrroline *N*-oxide (DMPO) (reaction (3)):

$$H_2O_2 \xrightarrow{\text{photolysis}} 2^{\bullet}OH \quad (2)$$

$$DMPO + {}^{\bullet}OH \rightarrow DMPO - {}^{\bullet}OH \quad (3)$$

A four-line spectrum (control) was obtained (Fig. 5A), showing hyperfine splitting constants of $\alpha_N = \alpha_H = 14.9$ G, a characteristic feature for the DMPO–$^{\bullet}OH$ spin adduct [35,41]. Fig. 5B shows the kinetics of the formation of DMPO–$^{\bullet}OH$ spin adduct in the photolysis of H_2O_2. As shown (Fig. 5B), for each M10 concentration used there was an increase in the amount of DMPO–$^{\bullet}OH$ production as a function of UV irradiation time. However, both the kinetics of $^{\bullet}OH$ formation and the maximum amplitude of the spin adduct signal were found to decrease as M10 concentration increased, with the formation of DMPO–$^{\bullet}OH$ being greatly suppressed at the higher concentration of M10 (Fig. 5B and d). Fig. 5C shows the inhibitory activity of M10 on DMPO–$^{\bullet}OH$ formation in the photolysis of H_2O_2. According to Fig. 5C, the IC_{50} for M10 was estimated to be about 0.3 molar ratio of M10 to H_2O_2 under the employed conditions. Considering that 1 molar H_2O_2 can produce 2 molar $^{\bullet}OH$ (reaction (2)), the IC_{50} value (0.3) implies that to reduce 50% of hydroxyl radical ($^{\bullet}OH$, 1 equivalent) produced by H_2O_2 only about 0.15 equivalents of M10 are needed. Together, these results indicate that M10 is a highly potent $^{\bullet}OH$ scavenger.

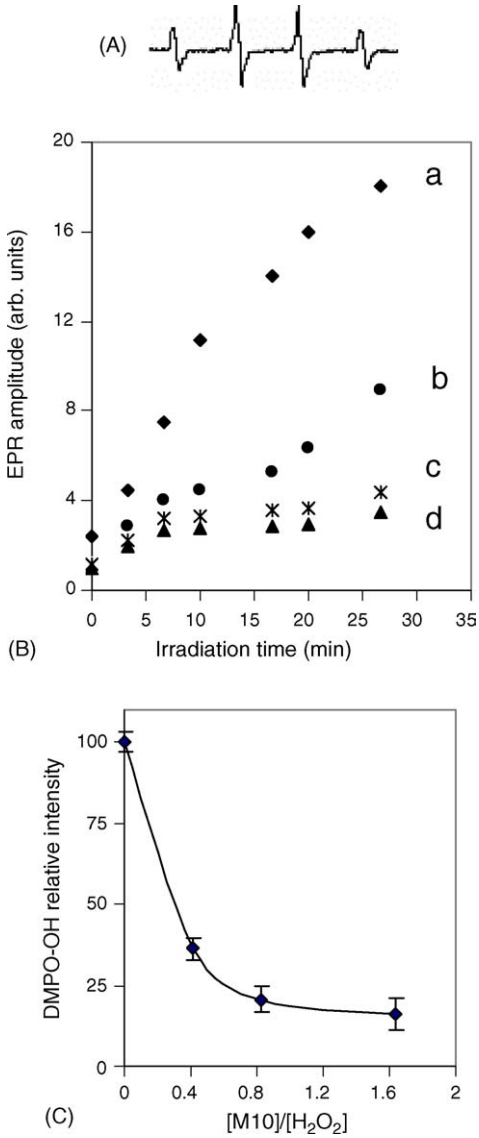

Fig. 5. (A) The EPR spectra of DMPO–$^{\bullet}OH$ spin adduct obtained by the photolysis of 2 mM H_2O_2 in HEPES buffer (pH 7.4) containing 50 mM DMPO with irradiation time of 10 min. The spectra are of DMPO–$^{\bullet}OH$, $a_N = a_H = 14.9$ G. (B) Kinetics of the formation of DMPO–$^{\bullet}OH$ spin adduct in the photolysis of 2 mM H_2O_2 in HEPES buffer (pH 7.4) at RT containing: (a) control; (b) 0.312 mM M10; (c) 0.625 mM M10; (d) 1.25 mM. (C) Inhibition on DMPO–$^{\bullet}OH$ formation by M10 in the photolysis of 2 mM H_2O_2 in HEPES buffer (pH 7.4) at RT.

4.4. Protective effects on 6-hydroxydopamine-induced toxicity in PC12 cells

The protective effects of M10 against 6-OHDA-induced apoptosis in PC12 are shown in Fig. 6. For comparison, this figure also presents the protection exerted by M9 (D-isomer of M10) and rasagiline (*N*-propargyl-1-(*R*)-aminoindan, Azilect, Agilect), a new generation of selective monoamine oxidase inhibitors, approved in Israel and Europe and

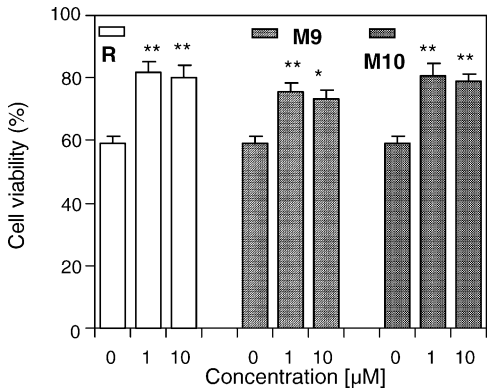

Fig. 6. Protective effects by rasagiline (R), M9 and M10 against 6-OHDA-induced toxicity in PC12 cells. PC12 cells (1×10^4 cells/well) in medium with one third of full serum content were incubated for 24 h and then pretreated with the indicated concentrations of the tested compounds 30 min before the addition of 6-OHDA (150 μM). Cell viability was assayed with MTT after 24 h incubation. Data are means ± S.E.M. of the percentage control, $n = 5$, $^{*}p < 0.05$, $^{**}p < 0.01$, compared with control.

has received a letter of approval from FDA for the treatment of PD [44,67,68]. As shown, both M10 and its D-isomer M9 afforded protection against cell death, with approximately the same protective activity. The maximum protective effects were observed with M10 and its D-isomer M9 at 1 μM. At that concentration, they exhibited about the same protective potency as rasagiline, with cell survival being increased to 82 ± 1% (R), 81 ± 2% (M10) and 75 ± 4% (M9), as compared with 59 ± 2% of the control.

4.5. Inhibitory effects on PC12 cell apoptosis induced by serum-deprivation

To further investigate and validate the neuroprotective action of M10, its effects against PC12 cell death induced by serum-free medium were also examined [42,43]. The anti-Parkinson drug rasagiline has been shown to be effective in attenuating PC12 cell death induced by serum-free medium [44]. In these experiments, rasagiline at a concentration of 10 μM reduced cell death from 100 ± 6% (control) to 70 ± 5%. At the same concentration, M 10 and its D-isomer decreased cell death to 67 ± 4 and 69 ± 1%, respectively (Fig. 7). At a lower concentration (1 μM) they were less potent than rasagiline in protecting against the PC12 cell death (Fig. 7). At this concentration, M10 showed slightly better protective activity than M9.

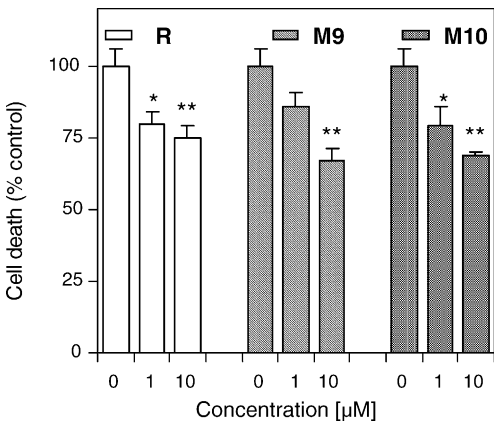

Fig. 7. Inhibitory effects of R (rasagiline), M9 and M10 on PC12 cell death induced by serum-free medium. Cells (0.3×10^4 cells/well) were placed in serum free containing 0.1% BSA. The tested drugs with the indicated concentrations were added and cell death was measured with ELISA assay after 24 h incubation. Data are means ± S.E.M., $n = 5$, $^{*}p < 0.05$, $^{**}p < 0.01$ as compared with control.

5. Discussion

This study describes the synthesis and evaluation of a novel antioxidant metal chelator (M10) on an amino acid carrier with a potential targeting to the brain. As a metal chelator, M10 forms stable complexes with Fe(III), Fe (II), Cu(II) and Zn(II) in HEPES buffer (pH 7.4) at 37 °C. These properties (capabilities) are of importance in biological systems. It is known that the oxygen radical superoxide ($O_2^{\bullet -}$) and hydrogen peroxide (H_2O_2) are produced during normal metabolism [45]. H_2O_2 can be rapidly decomposed via the Fenton reaction [45]:

$$Fe^{2+} + H_2O_2 \rightarrow Fe^{3+} + {}^{\bullet}OH + OH^- \quad (4)$$

In addition, oxygen radical superoxide ($O_2^{\bullet -}$) and hydrogen peroxide (H_2O_2), as well as the hydroxyl radical ($^{\bullet}OH$) can be interconverted via the so-called Haber–Weiss reaction:

$$\begin{array}{l} Fe^{3+} + O_2^{\cdot -} \leftrightarrow Fe^{2+} + O_2 \\ \underline{Fe^{2+} + H_2O_2 \rightarrow Fe^{3+} + {}^{\cdot}OH + OH^-} \\ O_2^{\cdot -} + H_2O_2 \rightarrow {}^{\cdot}OH + OH^- + O_2 \end{array} \quad (5)$$

Cuprous and cupric ions may substitute for ferrous and ferric ions in the Haber–Weiss reaction [45]. The produced free radicals, especially the highly toxic hydroxyl radical ($^{\bullet}OH$), exacerbate oxidative stress which causes damage to DNA, lipids, proteins and ultimately cell death associated with PD and other neurodegenerative diseases [4,6,15,16,45]. Iron may have a direct impact on plaque formation through its effects on amyloid precursor protein (APP) [46], and may be also closely linked to the proliferation of the reactive microglia and the inflammatory responses observed in neurotoxin-induced neurodegeneration and neurodegenerative diseases [18,19,47]. In addition, both zinc and copper, like iron, are markedly elevated in the AD brain, reaching high concentrations especially in Aβ deposits in humans and in APP transgenic mice that model AD-like Aβ amyloidosis [48,49].

Aβ is rapidly precipitated by Zn^{2+} even at low-physiological (sub-micromolar) concentrations [50]. Cu^{2+} and Fe^{3+}also induce marked Aβ aggregation. Significantly, Aβ, when bound to Cu^{2+} or Fe^{3+}, reduces the metal ions and produces H_2O_2, a substrate for the Fenton reaction that

generates the highly reactive hydroxyl radical (•OH) [51]. Consequently, like iron chelator, Zn/Cu chelators by binding to Zn/Cu would potentially be able to limit oxidation injury and Aβ aggregation, and thus enhance neurological recovery. Indeed, oral administration of the Cu/Zn chelator clioquinol, a drug withdrawn from the market because of its toxicity [24], induces 49% decrease in brain β-amyloid deposition in AD transgenic mouse [23].

M10 forms iron-complexes in HEPES buffer (pH 7.4) with $\log K_{1\ \text{for Fe(II)}} = 5.07 \pm 0.31$ and $\log K_{3\ \text{for Fe(III)}} = 12.25 \pm 0.55$, values which are below that of transferrin ($\log K = 20$ at pH 7.4) [52]. Therefore, it is expected that M10 would not cause iron mobilization from this protein and thus avoid undesirable side effects. In fact, previous studies have shown that the neuroprotective iron chelator VK-28, which has the same chelating backbone (qinoline) and a similar iron binding capacity to that of M10, does not alter peripheral iron metabolism when applied per os (p.o.) or intramuscularly (i.m.). VK28 treatment has no net effects on the iron-dependent rate limiting enzymes tyrosine hydroxylase and tryptophan hydroxylase [30].

Although the novel chelator M10 has a lower affinity for iron than that of DFO, it is highly inhibitory against iron-induced lipid peroxidation, with an IC_{50} value (12 μM) comparable to that of DFO. The high affinity of DFO for iron precludes its use for prolonged period of time in cases unrelated to iron overload due to serious cytotoxicity [26,27]. The cytotoxicity of DFO is very likely attributed to its interaction with iron containing enzymes and proteins, resulting in iron mobilization from these compounds [27].

The remarkable inhibition of M10 on LPO can be explained by its iron chelating property that interferes with the Fenton reaction, resulting in a decrease in hydroxyl free radical production. However, like other antioxidants, M10 may also act as a free radical scavenger to show its inhibitory activity. Indeed, our EPR study on M10 confirmed this hypothesis. It is known that the formation of •OH by H_2O_2 photolysis is iron-independent and can be catalyzed by UV light [35]. M10 significantly decreased the intensity of the DMPO–•OH signal produced in the photolysis of H_2O_2 (as shown in Fig. 5B and C), suggesting that it acts as a radical scavenger to directly scavenge •OH.

The neuroprotective activity of the novel chelator M10 was investigated using PC12 cell models. PC12 cells possess properties associated with neuroblasts and neurons and constitute a useful model for studying the mechanism of neuronal apoptosis [42,43]. Two PC12 cell models (serum-deprived and 6-OHDA-induced cell death) have been widely used in studies of neuronal cell survival and death. It has been demonstrated that, when serum is removed from the culture medium, PC12 cells die and exhibit the characteristic pattern of DNA fragmentation associated with apoptosis [42,43]. 6-OHDA also induces apoptosis in PC12 cells, which secrete dopamine and possess a dopamine transporter [54,65]. 6-OHDA is a neurotoxin for catecholaminergic cells, and it can reproduce PD-like cell damage in vivo. In vitro, PC12 cell death induced by 6-OHDA is thought to be related to oxidative stress [66]. Numerous laboratories have used them as a model of neurons and neurodegeneration [54,65]. Our studies have shown that M10 displays potent neuroprotective activity, which is comparable to that of the structurally similar chelator M30 in serum-free and 6-OHDA PC12 cell models and prevents cell death at concentrations as low as 1 μM [39,40]. M9 (D-isomer of M10) showed similar protective effects in the same experiments (Figs. 6 and 7). However, M10 is expected to have advantage over M30 in possessing a neutral amino acid carrier (system L), selectively targeted to the brain. Our results also suggest that the neuroprotection offered by M10 and M9 may be mediated by its iron chelating and antioxidative properties since both M10 and M9 have similar iron chelating potency and antioxidant-radical scavenging activities. Both serum free and 6-OHDA related neurotoxicity can be attributed to oxidative stress since they significantly enhance the level of ROS in PC12 cells and in rat cortical neurons [53]. Moreover, ROS related oxidative stress or/and 6-OHDA itself can initiate iron release from its inert storage site in ferritin into the labile toxic pool [15,16,54]. The redox iron released from ferritin via the Fenton reaction exacerbates oxidative stress associated with cell death [9,54]. In fact, previous studies have shown that iron chelators, such as DFO and VK-28, can bind iron to form stable iron-complexes which block the •OH radical production via the Fenton reaction, and therefore protect against oxidative stress-induced cell death [20,21,30]. Also, free radical scavenging antioxidants such as reduced glutathione, *N*-acetyl-cystyeine, or dithiothreitol, protect PC12 cells against oxidative stress by directly scavenging free radicals [55,56].

We have shown that M10 is a potent metal chelator with highly free radical scavenging potency. These features render it highly advantageous since studies have shown that treatment with both a radical scavenger and an Fe-chelator protect brain tissue from oxidative stress to a greater degree than is achievable with either a radical scavenger or an Fe-chelator alone. Moreover, a ''hybrid'' molecule possessing both radical scavenging and Fe-chelating ability is more effective in protecting brain tissue from oxidative stress than is achievable with combined administration of single-action molecules [57–60].

M10 is a water-soluble molecule with a log *D* (logarithm of the *n*-octanol/water distribution coefficients) less than −2 [61]. Thus, it is expected that M10 would not easily cross-cellular barriers by passive diffusion, which favors lipophilic molecules. In fact, preliminary studies have shown that M10 has low permeability through K562 cells, erythroleukemia cell lines which have been extensively studied in terms of their iron-regulatory properties [61–63]. The low diffusion of M10 into cells may help prevent its interference with the normal intracellular iron metabolism

and thus reduce the drug toxicity. Possible penetration of M10 into the brain would not occur through the passive diffusion pathway but rather via specific carrier-mediated transporter, given that M10 possesses a neutral amino acid carrier (system L) selectively targeting to the brain. System L, which is located in brain capillary endothelium, is known to facilitate the brain uptake of a series of hydrophilic amino acids or amino acid drugs such as L-DOPA, α-methyl-DOPA, azaserine, melphalan, 6-diazo-5-oxo-L-norleucine, acivicin, norleucine, acivicin and SDZ EAB 515 [31–34,64]. Studies are underway to examine the in vivo bioavailability of M10 in the brain and evaluate its neuroprotective activities in mice MPTP model of Parkinson's disease.

Acknowledgements

M.F. is a Lester Pearson Professor of Protein Chemistry. We are grateful to the Technion-Research and Development (Haifa, Israel), the National Parkinson Foundation (Miami, USA) and the Michael J. Fox Foundation (New York, USA) for supporting this work. We are grateful to Ms Orit Bar-Am and Shunit Gal for technical assistance. We also thank Mr Yigal Avivi for editing the manuscript.

References

[1] McDowell I. Alzheimer's disease: insights from epidemiology. Aging 2001;13:143–62.
[2] Drukarch B, van Muiswinkel FL. Drug treatment of Parkinson's disease. Time for phase II. Biochem Pharmacol 2000;59:1023–31.
[3] Dunnett SB, Bjorklund A. Prospects for new restorative and neuroprotective treatments in Parkinson's disease. Nature 1999;399:A32–9.
[4] Mandel S, Grunblatt E, Riederer P, Gerlach M, Levites Y, Youdim MBH. Neuroprotective strategies in Parkinson's disease: an update on progress. NS Drugs 2003;17:729–62.
[5] Sen CK. Redox signaling and the emerging therapeutic potential of thiol antioxidants. Biochem Pharmacol 1998;55:1747–58.
[6] Gilgun-Sherki Y, Melamed E, Offen D. Oxidative stress induced-neurodegenerative diseases: the need for antioxidants that penetrate the blood–brain barrier. Neuropharmacol 2001;40:959–75.
[7] Gilgun-Sherki Y, Rosenbaum Z, Melamed E, Offen D. Antioxidant therapy in acute central nervous system injury: current state. Pharmacol Rev 2002;54:271–84.
[8] Zecca L, Youdim MB, Riederer P, Connor JR, Crichton RR. Iron, brain, ageing and neurodegenerative disorders. Nat Rev Neurosci 2004;5:863–73.
[9] Takanashi M, Mochizuki H, Yokomizo K, Hattori N, Mori H, Yamamura Y, et al. Iron accumulation in the substantia nigra of autosomal recessive Juvenile parkinsonism (ARJP). Parkinson's Relat Disord 2001;7:311–4.
[10] Jellinger KA. The role of iron in neurodegeneration: prospects for pharmacotherapy of Parkinson's disease. Drugs Aging 1999;14:115–40.
[11] Shults MD, Pearce DA, Imperiali B. Modular and tunable chemosensor scaffold for divalent zinc. J Am Chem Soc 2003;125:10591–7.
[12] Walkup GK, Imperiali B. Stereoselective synthesis of fluorescent-amino acids containing oxine (8-hydroxyquinoline) and their peptide incorporation in chemosensors for divalent zinc. J Org Chem 1998; 63:6727–31.
[13] Mattson MP. Metal-catalyzed disruption of membrane protein and lipid signalling in the pathogenesis of neurodegenerative disorders. Ann NY Acad Sci 2004;1012:37–50.
[14] Przedborski S, Jackson-Lewis VR. ROS and Parkinson's disease: a view to a kill. Oxidative Stress Dis 2000;5:273–90.
[15] Desport JC, Couratier P. Oxidative stress in neurodegenerative diseases. Nutr Clin Metab 2002;16:253–9.
[16] Huang X, Cuajungco MP, Atwood CS, Moir RD, Tanzi RE, Ashley I, et al. Alzheimer's disease, β-amyloid protein and zinc. J Nutr 2000; 130:1488S–92S.
[17] Rottkamp CA, Raina AK, Zhu X, Gaier E, Bush AI, Atwood CS, et al. Redox-active iron mediates amyloid-β toxicity. Free Radic Biol Med 2001;30:447–50.
[18] Shoham S, Youdim MBH. Iron involvement in neural damage and microgliosis in models of neurodegenerative diseases. Cell Mol Biol 2000;46:743–60.
[19] Ben-Shachar D, Eshel G, Finberg JP, Youdim MBH. The iron chelator desferrioxamine (Desferal) retards 6-hydroxydopamine-induced degeneration of nigrostriatal dopamine neurons. J Neurochem 1991;56:1441–4.
[20] Lan J, Jiang DH. Desferrioxamine and Vitamin E protect against iron and MPTP-induced neurodegeneration in mice. J Neural Transm 1997; 104:469–81.
[21] Kaur D, Yantiri F, Rajagopalan S, Kumar J, Mo JQ, Boonplueang R, et al. Genetic or pharmacological iron chelation prevents MPTP-induced neurotoxicity in vivo: a novel therapy for Parkinson's disease. Neuron 2003;37:899–909.
[22] Cherny RA, Atwood CS, Xilinas ME, Gray DN, Jones WD, McLean CA, et al. Treatment with a copper–zinc chelator markedly and rapidly inhibits β-amyloid accumulation in Alzheimer's disease transgenic mice. Neuron 2001;30:665–76.
[23] Arasaki K, Nakanishi T. Selective neurotoxicity of clioquinol on the function of the posterior column nuclei. Neurosci Lett 1989;107:85–8.
[24] Porter JB, Huens ER. The toxic effects of desferrioxamine. Bailliere's Clin Haematol 1989;2:459–74.
[25] Singh S, Khodr H, Taylor MI, Hider RC. Therapeutic iron chelators and their potential side effects. Biochem Soc Symp 1996;61:127–37.
[26] Waldmeier PC, Buchle AM, Steulet AF. Inhibition of catechol-*O*-methyltrans-ferase (COMT) as well as tyrosine and tryptophane hydroxylase by the orally active iron chelator, 1,2-dimethyl-3-hydroxypyridin-4-one (L1, CP20), in rat brain in vivo. Biochem Pharmacol 1993;45:2417–24.
[27] Warshawsky A, Ben-Shachar D, Youdim MBH. Pharmaceutical compositions comprising iron chelators for the treatment of neurodegenerative disorders and some novel iron chelators. International application published under the patent cooperation treaty; 2000 [International Publication Number WO 00/74664 A2].
[28] Warshawsky A, Youdim MBH, Fridkin M, Zheng H, Warshawsky R. Preparation of neuroprotective iron chelators and pharmaceutical compositions comprising them; 2004 [Int. Publication Number WO 2004041151, A2 20040521].
[29] Ben-Shachar D, Nava Kahana N, Kampel V, Warshawsky A, Youdim MHB. Neuroprotection by a novel brain permeable iron chelator, VK-28, against 6-hydroxy-dopamine lession in rats. Neuropharmacol 2004;46:254–63.
[30] Zheng H, Weiner LM, Bar-Am O, Epsztejn M, Cabantchik I, Warshawsky A, et al. Design, synthesis and evaluation of novel bifunctional iron-chelators as potential agents for neuroprotection in neurodegenerative diseases. Bioorg Med Chem 2005;13:773–83.
[31] van Bree JBMM, Audus KL, Borchardt RT. Carrier-mediated transport of baclifen across monolayers of bovine brain endothelial cells in primary culture. Pharm Res 1988;5:369–71.
[32] Takada Y, Vistica DT, Greig NH, Purdon D, Rapoport SI, Smith QR. Rapid high-affinity transport of a chemotherapeutic amino acid across the blood–brain barrier. Cancer Res 1992;52:2191–6.

[33] Greig NH, Momma S, Sweeney DJ, Smith QR, Rapoport SI. Facilitated transport of melphalan at the rat blood–brain barrier by the large neutral amino acid carrier system. Cancer Res 1987;47:1571–6.
[34] Li JH, Bigge CF, Williamson RM, Borosky SA, Vartanian MG, Ortwine DF. Potent, orally active, competitive *N*-methyl-D-aspartate (NMDA) receptor antagonists are substrates for a neutral amino acid uptake system in Chinese hamster ovary cells. J Med Chem 1995; 38:1955–65.
[35] Harbour JR, Chow V, Bolton JR. An electron spin resonance study of the spin adducts of $^{\bullet}OH$ and $HO_2^{\bullet}$ radicals with nitrones in the ultraviolet photolysis of aqueous hydrogen peroxide solutions. Can J Chem 1974;52:3549–53.
[36] Gassen M, Glinka Y, Pinchasi B, Youdim MBH. Apomorphine is a highly potent free radical scavenger in rat brain mitochondrial fraction. Eur J Pharmacol 1996;308:219–25.
[37] Job P. Formation and stability of inorganic complexes in solution. Ann Chim 1928;9:113–203.
[38] Foley R, Anderson RC. Spectrophotometric studies of complex formation with sulfosalicylic acid. II. With uranyl ion. J Am Chem Soc 1949;71:909–12.
[39] Zheng H, Gal S, Weiner LM, Bar-Am O, Warshawsky A, Fridkin M, et al. Novel multifunctional neuroprotective iron chelator-monoamine oxidase drugs for neurodegenerative diseases. I. In vitro studies on antioxidant activity, prevention of lipid peroxide formation and monoamine oxidase inhibition. J Neurochem 2005;95:68–78.
[40] Gal S, Zheng H, Fridkin M, Youdim MBH. Novel multifunctional neuroprotective iron chelator-monoamine oxidase inhibitor drugs for neurodegenerative diseases. II. In vivo selective brain monoamine oxidase inhibition and neuro-protective activity. J Neurochem 2005; 95:79–88.
[41] Weiner LM. Quantitative determination of thiol groups in low and high molecular weight compounds by electron paramagnetic resonance. Meth Enzymol 1995;251:87–105.
[42] Rukenstein A, Rydel RE, Greene LA. Multiple agents rescue PC12 cells from serum-free cell death by translation- and transcription-independent mechanisms. J Neurosci 1991;11:2552–63.
[43] Greene LA. Nerve growth factor prevents the death and stimulates the neuronal differentiation of clonal PC12 pheochromocytoma cells in serum-free medium. J Cell Biol 1978;78:747–55.
[44] Youdim MBH, Weinstock M. Novel neuroprotective anti-Alzheimer drugs with anti-depressant activity derived from the anti-Parkinson drug, rasagiline. Mech Aging Dev 2002;123:1081–6.
[45] Halliwell B. Reactive oxygen species and the central nervous system. J Neurochem 1992;59:1609–23.
[46] Rogers JT, Randall JD, Cahill CM, Eder PS, Huang XD, Hiromi Gunshin H, et al. An iron-responsive element type II in the 5′-untranslated region of the Alzheimer's amyloid precursor protein transcript. J Biol Chem 2002;277:45518–28.
[47] Hunot S, Brugg B, Ricard D, Michel PP, Muriel MP, Merle Ruberg M, et al. Nuclear translocation of NF-kappaB is increased in dopaminergic neurons of Patients with Parkinson disease. Proc Natl Acad Sci USA 1997;94:7531–6.
[48] Lovell MA, Robertson JD, Teesdale WJ, Campbell JL, Markesbery WR. Copper, iron and zinc in Alzheimer's disease senile plaques. J Neurol Sci 1998;158:47–52.
[49] Suh SW, Jensen KB, Jensen MS, Silva DS, Kesslak JP, Danscher G, et al. Histological evidence implicating zinc in Alzheimer's disease. Brain Res 2000;852:274–8.
[50] Bush AI, Pettingell WH, Multhaup G, Paradis MD, Vonsattel J-P, Beyreuther K, et al. Rapid induction of Alzheimer A βamyloid formation by zinc. Science 1994;265:1464–7.
[51] Smith MA, Perry G, Richey PL, Sayre LM, Anderson VE, Beal MF, et al. Oxidative damage in Alzheimer's disease. Nature 1996;382: 120–121.
[52] Kretchmar Nguyen SA, Craig A, Raymond KN. Transferrin: the role of conformational changes in iron removal by chelators. J Am Chem Soc 1993;115:6758–64.
[53] Atabay C, Cagnoli CM, Kharlamov E, Ikonomovic MD, Manev H. Removal of serum from primary cultures of cerebellar granule neurons induces oxidative stress and DNA fragmentation: protection with antioxidants and glutamate receptor antagonists. J Neurosci Res 1996;43:465–75.
[54] Glinka Y, Gassen M, Youdim MBH. Mechanism of 6-hydroxydopamine neurotoxicity. Adv Res Neurodegen 1997;5:55–66.
[55] Offen D, Ziv I, Sternin H, Melamed E, Hochman A. Prevention of dopamine-induced cell death by thiol antioxidants: possible implications for treatment of Parkinson's disease. Exp Neurol 1996;141: 32–39.
[56] Chiou TJ, Tzeng WF. The roles of glutathione and antioxidant enzymes in menadione-induced oxidative stress. Toxicology 2000; 154:75–84.
[57] Bebbington D, Monck NJT, Gaur S, Palmer AM, Benwell K, Harvey V, et al. 3,5-Disubstituted-4-hydroxyphenyls linked to 3-hydroxy-2-methyl-4(1H)-pyridinone: potent inhibitors of lipid peroxidation and cell toxicity. J Med Chem 2000;43:2779–82.
[58] Dailly E, Urien S, Tillement JP. Chain-breaking antioxidants and ferriheme bound drugs are synergistic inhibitors of erythrocyte membrane peroxidation. Free Radic Res 1998;28:205–14.
[59] Ghaemy M, Fruzandeh S. Synergistic effects of some phosphites antioxidants used in polypropylene stabilization. Iran Polym J 1999;8:51–9.
[60] Xi F, Barclay LRC. Cooperative antioxidant effects of ascorbate and thiols with di-*tert*-butylcatechol during inhibited peroxidation in solution and in sodium dodecyl sulfate (SDS) micelles. Can J Chem 1998;76:171–82.
[61] Warshawsky A, Youdim M, Fridkin M, Zheng HL, Warshawsky R. Preparation of neuroprotective iron chelators and pharmaceutical compositions comprising them; 2004 [International Publication Number WO 2004041151 A2].
[62] Epsztejn S, Kakhlon O, Glickstein H, Breuer W, Cabantchik ZI. Fluorescence analysis of the labile iron pool of mammalian cells. Anal Biochem 1997;248:31–40.
[63] Zanninelli G, Glickstein H, Breuer W, Milgram P, Brissot P, Hider RC, et al. Chelation and mobilization of cellular iron by different classes of chelators. Mol Pharmacol 1997;51:842–52.
[64] Anderson BD. Prodrugs for improved CNS delivery. Adv Drug Deliver Rev 1996;19:171–202.
[65] Walkinshaw G, Waters CM. Neurotoxin-induced cell death in neuronal PC12 cells is mediated by induction of apoptosis. Neuroscience 1994;63:975–87.
[66] Grunblatt E, Mandel S, Youdim MBH. Neuroprotective strategies in Parkinson's disease using the models of 6-hydroxydopamine and MPTP. Ann NY Acad Sci 2000;899:262–73.
[67] Schapira A, Bate G, Kirkpatrick P. Fresh from the pipeline: rasagiline. Nat Rev Drug Discov 2005;4:625–6.
[68] Rascol O, Brooks DJ, Melamed E, Oertel W, Poewe W, Stocchi F, et al. Rasagiline as an adjunct to levodopa in patients with Parkinson's disease and motor fluctuations (LARGO, Lasting Effect in Adjunct Therapy with Rasagiline Given Once Daily, study): a randomized, double-blind, parallel-group trial. Lancet 2005; 365:947–54.